2009 Southern California Earthquake Center Annual Report
Systematic Analysis of Non-Volcanic Tremor in Southern California

Zhigang Peng (PI)
School of Earth and Atmospheric Sciences
Georgia Institute of Technology, Atlanta, GA, 30338
March 31, 2010

Summary

A systematic analysis of non-volcanic tremor in southern California could provide important new information on the fault mechanics on the deep extension of the crustal faults and may shed new light on the predictability of large earthquakes. Our past year's effort mainly focused on the following two directions: (1) systematic search of triggered tremor in California; and (2) high-frequency artifacts in the large-amplitude surface waves from analysis procedures.

Systematic search of triggered tremor in California

"Non-volcanic" tremor is a long-duration and emergent seismic signals observed away from volcanic regions. Since its first discovery in the subduction zone southwest of Japan (Obara, 2002), tremor was subsequently found at many places in circum-Pacific subduction zones (e.g., Peng and Gomberg, 2010; and reference therein), along the San Andears Fault (SAF) near Cholame (Nadeau and Dolenc, 2005; Nadeau and Guilhem, 2009; Shelly et al., 2009), and along the San Jacinto Fault (SJF) in Southern California (Hillers and Ampuero, 2009). Recent studies have found that in addition to occurring in protracted ETS episodes, tremor can be instantaneously triggered during the surface waves of large teleseismic events in subduction zones (Miyazawa and Brodsky, 2008; Miyazawa and Mori, 2005, 2006; Rubinstein et al., 2007, 2009), along the SAF in Central (Gomberg et al., 2008; Peng et al., 2008, 2009; Ghosh et al., 2009) and Southern California (Brown et al., 2009b; Wang and Cochran, 2009; Fabian et al., 2009), and beneath the Central Range in Taiwan, an arc-continental type collision environment (Peng and Chao, 2008; Chao et al., 2009).

Gomberg et al. (2008) conducted a systematic survey of tremor triggered by teleseismic waves of the 2002 Mw7.8 Denali Fault earthquake. They identified at least at least 7 places along the SAF in California that have generated clear tremor signals, including two places in southern California: the SJF near Hemet, and the Simi Valley. Fabian et al. (2009) performed a visual inspection of remotely triggered tremor in Northern and Southern California (Figure 1), focusing on the following regions with dense instrumentations: the Central Calaveras fault, the Northern Hayward fault, the SJF near Hemet and the Simi Valley, and the San Gabriel Mountains (SGM). Out of the 30 large teleseismic events with Mw $\geq$ 7.5 since 2001, only the 2002 Mw7.8 Denali Fault earthquake has triggered tremor in all these regions, including the SGM where neither triggered nor ambient tremor has been observed before. Our results suggest a relative lack of widespread triggering in Northern and Southern California (Figure 2), which is in contrast with the finding of multiple events that triggered tremor in Central California, Japan, Cascadia, and Taiwan. However, such observation is consistent with a general lack of ambient tremor activities in these regions, and another independent study by Wang and Cochran (2009). Recently, Aguiar et al. (2009) and Brown et al. (2009b) have detected several cases of triggered tremor by regional and teleseismic events around the SJF and the Calaveras fault based on the waveform matched filter technique (Brown et al., 2008, 2009a). The difference between their results and ours mainly

lie in the fact that we are using visual inspection to detect triggered tremor. Hence, we may omit weak triggered tremor signals that are close or below the background noise levels. The tremor observed near the Calaveras fault and SJF appears to be initiated by Love waves, and becomes intensified during the large amplitude Rayleigh waves (Figure 3). The tremor triggered in Simi Valley and SGM only shows weak correlations with the Rayleigh waves.

Perhaps a more convincing case is the triggered tremor associated with the 2010/02/28 Mw8.8 Chilean earthquake. This earthquake has triggered clear tremor in Central California near Cholame (Peng, 2010). However, a careful examination of data recorded by both the Anza and Caltech's Southern California Seismic Network (SCSN) and the borehole seismic stations in the Plate Boundary Observatory (PBO) fails to identify any clear triggered tremor in southern California near the SJF. The SJF is slightly closer to the Chilean epicenter than SAF near Cholame. Hence, the PGV and the associated dynamic stress would be slightly larger. In addition, the PBO borehole stations would be in the similar quality as the High Resolution Seismic Network (HRSN) borehole stations near Parkfield in central California. Hence, it is unlikely that the difference in triggering behavior can be purely explained by the network detection ability. Again, we suggest that variability in the background tremor rate or different tremor triggering threshold could be the main cause of the different behaviors.

High-frequency artifacts in the large-amplitude surface waves from analysis procedures

The second work on high-frequency artifact is not planed in the original proposal and is initiated by serendipity. In an effort (Fabian et al., 2009) to identify additional triggered tremor in Southern California (Figure 1b), we compute spectrograms from all the seismic records in the Southern California Earthquake Data Center (SCEDC) that are generated by the 2002 Mw7.8 Denali Fault earthquake, based on the Matlab's *spectrogram* and *specgram* command.

Figure 4 shows an example of the original 3-component broadband seismograms (HH channels), 2-16 Hz band-pass-filtered transverse component, and the corresponding spectrogram recorded by the station MWC near the Mount Wilson Observatory on the SGM. This station has recorded weak tremor triggered by the 2002 Denali Fault earthquake (Fabian *et al.*, 2009). A general pattern in the spectrogram from this and other stations equipped with broadband seismometer/digitizer systems is bursts of high-frequency energy during the large-amplitude surface waves. A zoom-in examination reveals that the high-frequency energy is mostly centered on the zero crossing in the broadband seismograms. In comparison, the spectrogram from the short-period recordings (EH channel) at the same station does not show elevated high-frequency energy during the long-period surface waves. Finally, such high-frequency energy is not shown in the 2-16 Hz band-pass-filtered seismograms. Hence, we suspect that such high-frequency signals are likely caused by the analysis procedures.

To further support the above hypothesis, we generate a synthetic seismogram from a pure sine function with 20-s period that mimics the typical 20-s surface waves with the same sampling rate (100/s). We find elevated high-frequency energy that is centered on the zero crossing of sine function (Figure 5), similar to the observations from the real data (e.g., Figure 1). This demonstrates that the high-frequency energy shown in the spectrogram must originate from the procedure to compute spectrograms from multiple short-time windows. Through additional synthetic example, we find that when the length of the window used to computed the FFT and the spectrogram is smaller than the wavelength of the seismic waves (i.e., during large-amplitude long-period surface waves), the windowing effect is amplified.

After we identify the cause of such high-frequency artifact, we propose the following three approaches (Figure 6) to remove or reduce such high-frequency artifacts: 1. Applying a high-pass

filter to reduce long period noises that cannot be resolved by the short-time windows; 2. Using narrow band-pass filtering (instead of short time windows) to compute the spectrogram; and 3. Computing the spectrum using the Burg method. All these approaches resulted in clean spectrogram that match the band-pass-filtered seismogram and the spectrogram from collocated short-period station well, suggesting that the aforementioned high-frequency artifact has been largely reduced. Because the spectrogram plot is useful to identify and demonstrate remotely triggered seismic activity (e.g., West *et al.*, 2005; Hill and Prejean, 2007; Peng and Chao, 2008; Peng *et al.*, 2008), it is important to identify such potential artifact, and use the proper approaches mentioned above to compute the correct spectrogram so that no false interpretation is made.

Student Support and Involvement. This project provided half-support for the GT graduate student Kevin Chao, who has become an export in studying triggered tremor in Taiwan, California, and New Zealand. In addition, this project supported two SCEC summer interns (Amanda Fabian and Lujendra Ojha) to help organize the data and perform the analysis. Both of them are well trained to conduct scientific research in the frontier of seismology, and have indicated their interest in continuing their career path within Geophysics. Such effects are valuable in attracting talented undergraduate students into the pipeline and preparing them for future challenges in the field of seismology.

References

Aguiar, A. C., J. R. Brown, and G. C. Beroza (2009), Non-volcanic tremor near the Calaveras Fault Triggered by Mw~8 Teleseisms, Eos Trans. AGU, 90(54), Fall Meet. Suppl., Abstract T23E-06.

Brown, J. R., G. C. Beroza, and D. R. Shelly (2008), An autocorrelation method to detect low frequency earthquakes within tremor, Geophys. Res. Lett., 35, L16305, doi:10.1029/2008GL034560.

Brown, J. R., G. C. Beroza, S. Ide, K. Ohta, D. R. Shelly, S. Y. Schwartz, W. Rabbel, M. Thorwart, and H. Kao (2009a), Deep low frequency earthquakes in tremor localize to the plate interface in multiple subduction zones, Geophys. Res. Lett., 36, L19306, doi:10.1029/2009GL040027.

Brown, J. R., A. C. Aguiar, and G. C. Beroza (2009b), Triggered tremor on the San Jacinto Fault from the 3 August 2009 Mw6.9 Gulf of California earthquake, 2009 SCEC Annual Meeting abstract, 242.

Chao, K., Z. Peng, C.-H. Lin, and C.-C. Tang (2009), Systematic analysis of triggered and ambient tremor beneath the Central Range in Taiwan, Eos Trans. AGU, 90(54), Fall Meet. Suppl., Abstract T11C-1821.

Fabian, A., L. Ojha, Z. Peng, and K. Chao (2009), Systematic search of remotely triggered tremor in Northern and Southern California, Eos Trans. AGU, 90(54), Fall Meet. Suppl., Abstract T13D-1916.

Ghosh, A., J. E. Vidale, Z. Peng, K. C. Creager and H. Houston (2009), Complex non-volcanic tremor near Parkfield triggered by the great 2004 Sumatra earthquake, J. Geophys. Res., doi:10.1029/2008JB006194.

Gomberg, J., J. L. Rubinstein, Z. Peng, K. C. Creager, and J. E. Vidale (2008), Widespread triggering of non-volcanic tremor in California, Science, 319, 173, doi: 10.1126/science.1149164.

Hill, D. P., and S. G. Prejean (2007). Dynamic triggering, in Treatise on Geophysics, 257–292, ed. Schubert, G., Vol. 4: Earthquake Seismology, ed. Kanamori, H., Elsevier, Amsterdam.

Hillers, G. and J. P. Ampuero (2009), Systematic search for spontaneous non-volcanic tremor in Southern California, Eos Trans. AGU, 90(54), Fall Meet. Suppl., Abstract T13D-1918.

Miyazawa, M. and E. E. Brodsky (2008), Deep low-frequency tremor that correlates with the passing surface waves, J. Geophys. Res., 113, B01307, doi:10.1029/2006JB004890, 2008.

Miyazawa, M., and J. Mori (2005), Detection of triggered deep low-frequency events from the 2003 Tokachi-oki earthquake, Geophys. Res. Lett., 32, L10307, doi:10.1029/2005GL022539.

Miyazawa, M., and J. Mori (2006), Evidence suggesting fluid flow beneath Japan due to periodic seismic triggering from the 2004 Sumatra-Andaman earthquake, Geophys. Res. Lett., 33, L05303, doi:10.1029/2005GL025087.

Nadeau, R. M., and D. Dolenc (2005), Nonvolcanic tremors deep beneath the San Andreas Fault, Science, 307, 389-389.

Nadeau, R. M. and A. Guilhem (2009), Nonvolcanic Tremor Evolution and the San Simeon and Parkfield, California, Earthquakes, Science, 325, 191-193.

Obara, K. (2002), Nonvolcanic deep tremor associated with subduction in southwest Japan, Science, 296, 1679-1681.

Peng, Z. (2010), Remote triggering of tremor and earthquakes in California following the 2010 Mw8.8 Chilean earthquake, Geophys. Res. Lett., in prep.

Peng, Z., and K. Chao (2008), Non-volcanic tremor beneath the Central Range in Taiwan triggered by the 2001 Mw7.8 Kunlun earthquake, Geophys. J. Int. (Fast track), doi: 10.1111/j.1365-246X.2008.03886.x.

Peng, Z. and J. Gomberg (2010). Slow slip phenomena in a global context. *Nature Geosci.*, in review.

Peng, Z., J. E. Vidale, K. C. Creager, J. L. Rubinstein, J. Gomberg, and P. Bodin (2008), Strong tremor near Parkfield, CA excited by the 2002 Denali Fault earthquake, Geophys. Res. Lett., 35, L23305, doi:10.1029/2008GL036080.

Peng, Z., J. E. Vidale, A. Wech, R. M. Nadeau and K. C. Creager (2009), Remote triggering of tremor along the San Andreas fault in central California, J. Geophys. Res., 114, B00A06, doi:10.1029/2008JB006049.

Rubinstein, J. L., J. E. Vidale, J. Gomberg, P. Bodin, K. C. Creager, and S. D. Malone (2007), Non-volcanic tremor driven by large transient shear stresses, Nature, 448, 579-582.

Rubinstein, J. L., J. Gomberg, J. E. Vidale, A. G. Wech, H. Kao, K. C. Creager, and G. Rogers (2009), Seismic wave triggering of nonvolcanic tremor, episodic tremor and slip, and earthquakes on Vancouver Island, J. Geophys. Res., 114, B00A01, doi:10.1029/2008JB005875.

Shelly, D. R., W. L. Ellsworth, T. Ryberg, C. Haberland, G. S. Fuis, J. Murphy, R. M. Nadeau, and R. Bürgmann (2009), Precise location of San Andreas Fault tremors near Cholame, California using seismometer clusters: Slip on the deep extension of the fault?, Geophys. Res. Lett., 36, L01303, doi:10.1029/2008GL036367.

Wang, T., and E. S. Cochran (2009), Study of triggered tremor characteristics and triggering threshold in Anza region, Southern California, Eos Trans. AGU, 90(54), Fall Meet. Suppl., Abstract T13D-1917.

West, M., J. J. Sanchez, and S. R. McNutt (2005). Periodically triggered seismicity at Mount Wrangell, Alaska, after the Sumatra earthquake. *Science* **308**, 1144–1146; doi:10.1126/science.1112462.

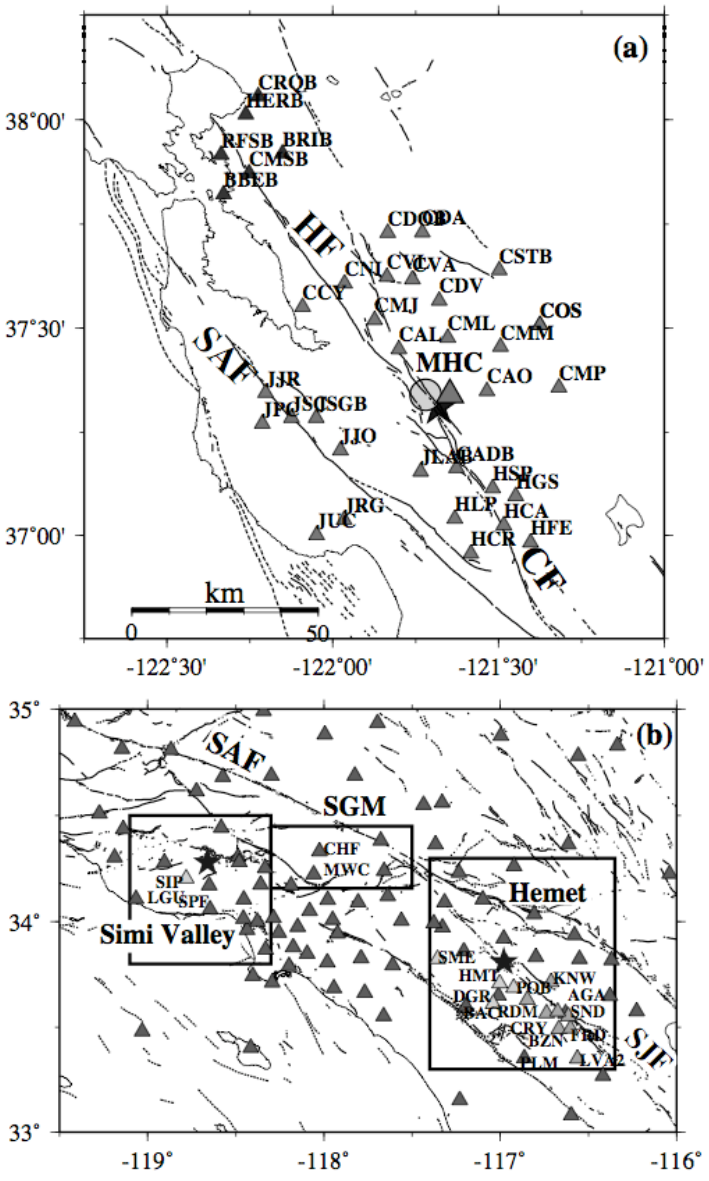

Figure 1. Map of study region in northern (a) and southern (b) California. The triangles mark the regional seismic network, and the gray lines mark the active faults. The stars represent previously determined tremor locations triggered by the Denali earthquake (Gomberg et al., 2008).

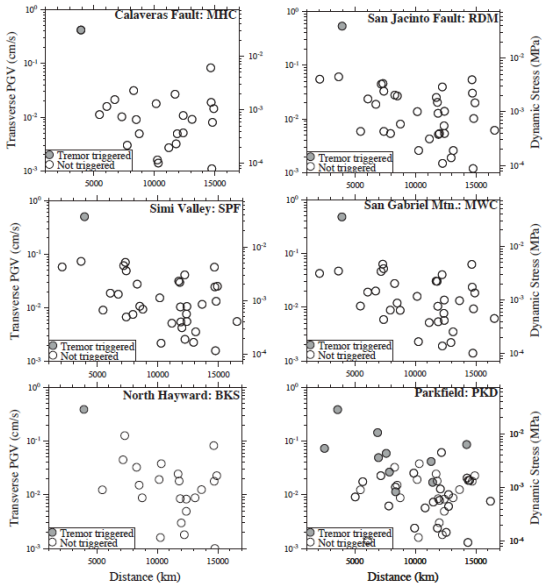

Figure 2. Peak ground velocities (left vertical axis) and related dynamic stresses (right vertical axis) for the transverse components measured at broadband stations in each studied region of California, plotted against the distance from the event to the station specified on plot label. Gray circles are events that caused tremor to be triggered in that area, open circles are events that did not trigger tremor.

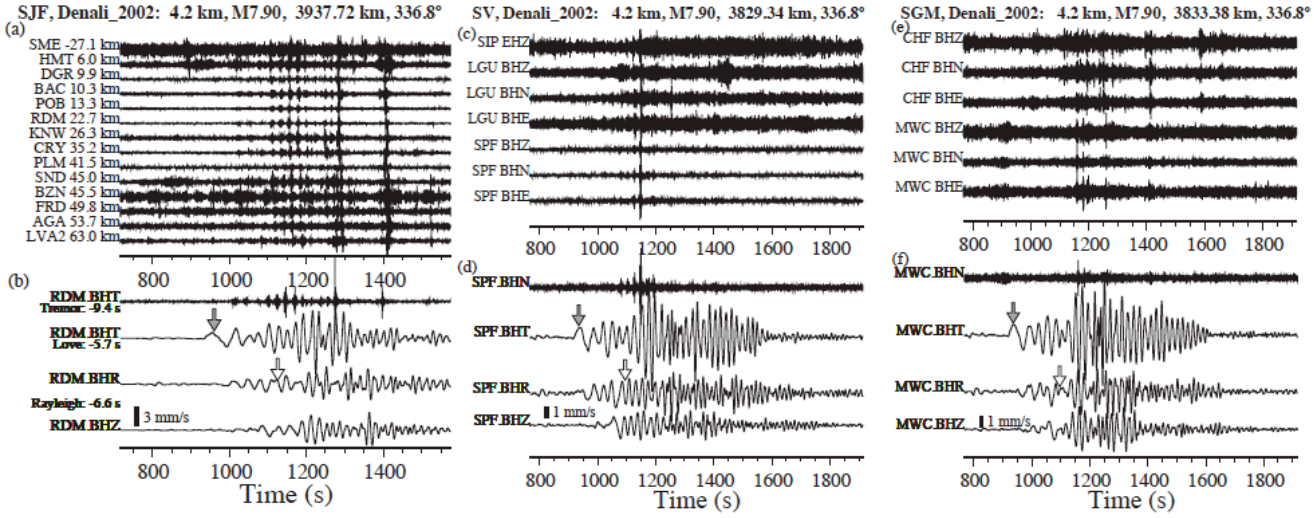

Figure 3. 2-8 Hz band-pass-filtered seismograms showing tremor triggered by the Denali Fault earthquake in the San Jacinto Fault (SJF, a), Simi Valley (SV, c), and San Gabriel Mountain (SGM, e). The bottom three panels show instrument corrected transverse (BHT), radial (BHR), and vertical (BHZ) seismograms and band-pass-filtered seismogram at each region.

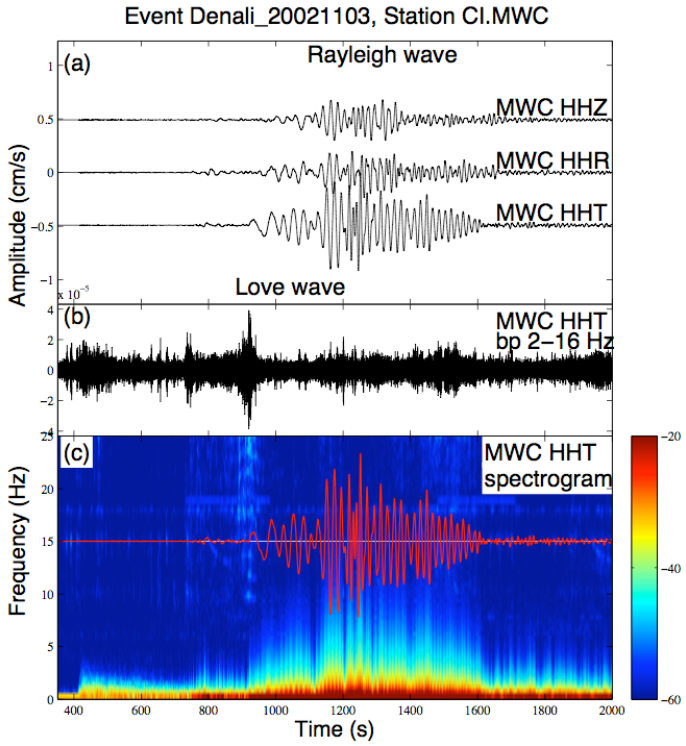

Figure 4. (a) Broadband 3-component seismograms generated by the 2002 Mw7.8 Denali Fault earthquake and recorded at the broadband station CI.MWC in Southern California. (b) 2-16 Hz band-pass-filtered transverse-component seismogram. (c) The spectrogram of the transverse-component seismogram at station CI.MWC shaded by the amplitude in db below the maximum.

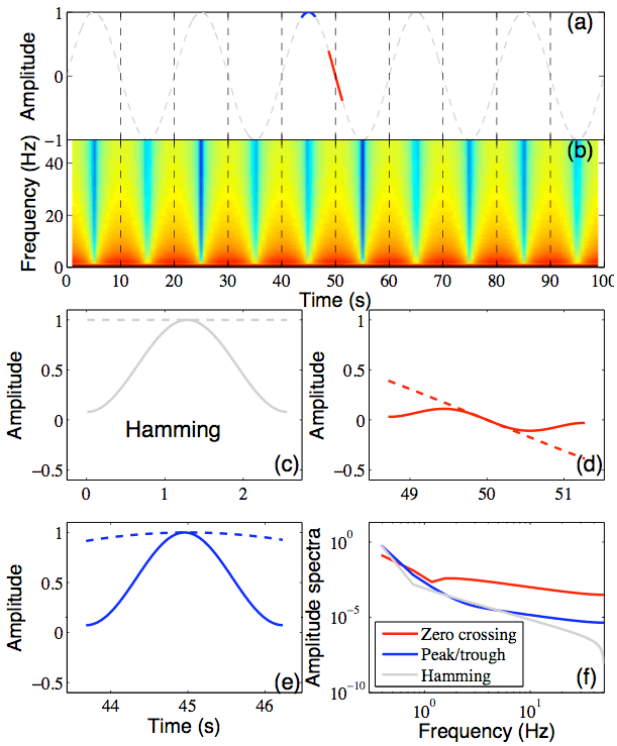

Figure 5. (a) A sine function with a period of 20 s. A Hamming window is applied to the segments marked with light gray (zero crossing) and black (peak/trough) respectively. (b) The spectrogram computed using the "*spectrogram*" command in *Matlab*^{R}. (c) The Hamming window (solid) and data with amplitude = 1 (dashed). (d) The truncated data around zero crossing (dashed) and after applying the Hamming window (solid). (e) The truncated data around the peak/trough (dashed) and after applying the Hamming window (solid). (f) The Fourier spectra of the Hamming window (light gray), the windowed zero crossing (gray), and windowed peak/trough (black).

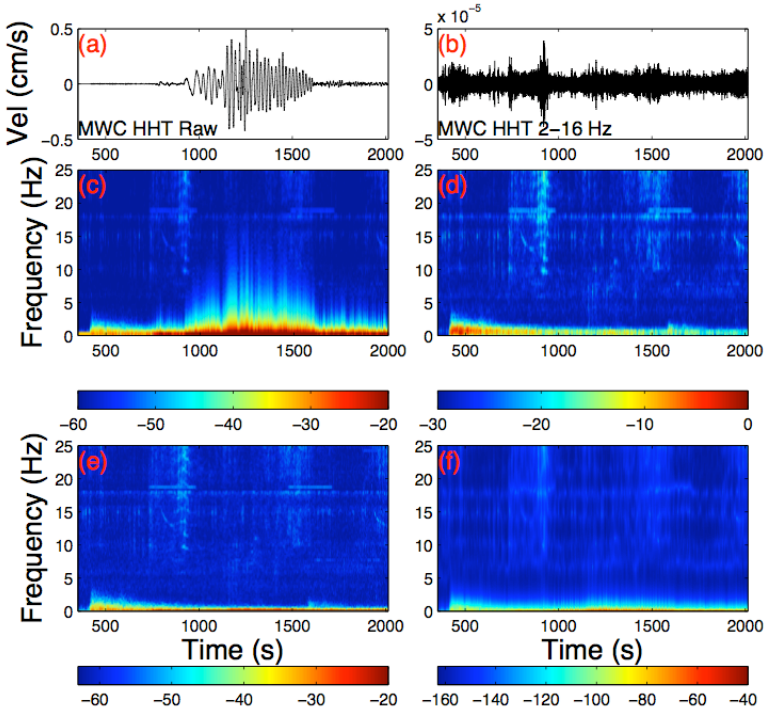

Figure 6. A comparison of the spectrogram for the transverse-component data at CI.MWC with and without corrections. (a) The spectrogram without correction. The raw data is plotted at 15 Hz for comparison. (b) The spectrogram after applying the 0.5 Hz high-pass-filter to the data. (c) The spectrogram computed from the multiple band-pass-filter technique. (d) The spectrogram from the Burg method.